A Comparative Study on the Electrical and Mechanical Behaviour of Multi-Walled Carbon Nanotube Composites Prepared by Diluting a Masterbatch With Various Types of Polypropylenes

Matej Mičušík,[1] Mária Omastová,[1] Igor Krupa,[2] Jan Prokeš,[3] Polycarpos Pissis,[4] Emmanuel Logakis,[4] Christos Pandis,[4] Petra Pötschke,[5] Jürgen Pionteck[5]

[1]*Slovak Academy of Sciences, Polymer Institute, Department of Composite Materials, Dúbravská cesta 9, 842 36 Bratislava, Slovakia*
[2]*Slovak Academy of Sciences, Polymer Institute, Department of Theoretical and Applied Research of Polymeric Materials, Dúbravská cesta 9, 842 36 Bratislava, Slovakia*
[3]*Charles University Prague, Faculty of Mathematics and Physics, Department of Macromolecular Physics, V Holesovickach 2, 182 00 Prague, Czech Republic*
[4]*National Technical University, Zografou Campus, Department of Physics, 157 80 Athens, Greece*
[4]*Leibniz Institute of Polymer Research Dresden, Department of Polymer Reactions and Blends, Hohe Str. 6, 01069 Dresden, Germany*

Received 29 September 2008; accepted 8 February 2009
DOI 10.1002/app.30418
Published online 28 April 2009 in Wiley InterScience (www.interscience.wiley.com).

ABSTRACT: Polypropylene (PP) nanocomposites with multi-walled carbon nanotubes (CNT) were produced by a small-scale masterbatch melt dilution technique using five PP differing in melt flow index (MFI) and degree of maleination. PP used in a masterbatch has MFI = 12 (PP_{12}), the others used PP which have MFI = 2 or MFI = 8. The state of CNT dispersion as assessed by melt rheological and morphological investigations indicated a better dispersion when using unmodified PP with MFI = 8 (PP_8) and the masterbatch's PP_{12}. Electrical conductivity results showed nanotube percolation at contents between 1.1 and 2.0 vol %, whereas lower values were obtained for the matrices with the best dispersion, i.e., PP_8 and PP_{12}. The dependencies of the relative Young's modulus on the CNT content showed that the maleinization improved the interfacial interactions between the components, especially in the case of maleated PP with MFI = 8 (PP-MA_8), but the better dispersion was prevented by the incompatibility between polar groups of PP-MA and the nonpolar origin masterbatch PP_{12}. © 2009 Wiley Periodicals, Inc. J Appl Polym Sci 113: 2536–2551, 2009

Key words: carbon nanotubes; nanocomposites; morphology; mechanical properties; rheology

INTRODUCTION

Due to their challenging structures and exceptional properties, carbon nanotubes (CNT) have attracted much attention of the academic and industrial researchers for the formation of electrical dissipative or conductive polymeric nanocomposites. The aims are to prepare antistatic or conductive composites with an extremely low value of percolation concentration, to conserve perfect mechanical properties of neat polymers or even improve large set of properties, including thermal conductivity, mechanical strength, etc. The theoretical as well as experimental results obtained from investigation of individual CNT give a justification to such notions. Depending on their structure, individual CNT exhibit extremely high mechanical strength, Young's modulus, and strain to failure as well as a remarkable electronic structure. Calculations and experimental measurements have determined that carbon nanotubes (especially single-walled CNT) possess excellent mechanical properties (tensile modulus about 1 TPa,[1] tensile strength from 11 to 63 MPa,[2] and compressive strength about 150 GPa) in the direction of the tubule axis. This could make them, theoretically, ideal as reinforcing fibres for the manufacture of the next generation of matrix composite materials.

Correspondence to: M. Mičušík (matej.micusik@savba.sk).
Contract grant sponsor: German-Slovak bilateral project "Electrical conductive nanocomposites"; contract grant number: D/05/15215.
Contract grant sponsor: Project of the Scientific Grant Agency of the Ministry of Education of Slovakia and the Slovak Academy of Sciences; contract grant number: VEGA 2/7103/27.
Contract grant sponsor: Scientific Grant Agency of the Ministry of Education of Slovak Republic and the Slovak Academy of Sciences; contract grant number: 2/0063/09.
Contract grant sponsor: Science and Technology Assistance Agency; contract grant number: APVV-0478-07.
Contract grant sponsor: The Ministry of Education, Youth, and Sports of the Czech Republic; contract grant number: MSMT 0021620834.

© 2009 Wiley Periodicals, Inc.

The research ambitions are focused on the preparation of materials having improved electrical conductivity and electrostatic discharging behaviour, flame-retardant performance, as well as high-thermal conductivity and high mechanical strength.[3,4] However, there are many problems which must be solved to satisfy those big expectations on CNT, which as typical colloidal material does not spontaneously suspend in polymers, thus the chemistry and physics of CNT dispersion is a major issue. Due to strong attractive interaction nanotubes have a tendency already during their synthesis to aggregate and form bundles or "ropes" that are very difficult to disrupt.[3] Ropes are tangled with one another like spaghetti or polymeric chains. With high shear, these ropes can be untangled, but it is extremely difficult to disperse them at the single tube level. Due to the low entropy of mixing, rigid molecules of high molecule weight require strong attractive interactions to disperse.[4] To ensure appropriate dispersion of carbon nanotubes within a polymeric matrix, the polymer-nanotube interface has to be properly modified. Various approaches have been proposed and studied. In general, they can be categorized as non-covalent surface modification and covalent surface modification of the nanotubes. Non-covalent surface modification is based on the van der Waals attraction between the nanotubes and various molecules.[5,6] The covalent modification of the nanotubes surface involves chemical reactions between the nanotube carbon atoms and the chemical reagents. These reactions cause changes in the walls of the nanotubes and, therefore, a loss in the perfectness of the original structure of the nanotubes.

The studies on the preparation of polymeric nanocomposites loaded by CNT have been based on three approaches: (1) mixing of CNT in polymer solutions,[7] (2) *in situ* polymerization of monomer/CNT mixtures,[8] and (3) melt blending (compounding) of CNT into polymer.[9] The first two approaches were mainly used for basic investigations of this class of nanocomposites and resulted in very promising results. Very low values of percolation concentration of CNT within epoxy matrices were reported as a consequence of excellent dispersion of CNT.[10,11] This is reached mainly by the low viscosity of the epoxy, appropriate functionalization of CNT, and very intensive ultra sonication of the mixture. However, it must be pointed out that in the case of epoxy matrices a sophisticated protocol of preparation of conductive composites can lead to extremely low values of percolation concentrations even in the case of traditional fillers as carbon black.[12,13] Obviously, the situation is much more complicated in the case of thermoplastic polymers as polyethylene, polypropylene, or polyamide mixed with CNT in the molten state, where ultrasonic dispersion is not applicable. These problems are similar to those with the preparation of thermoplastic nanocomposites filled with clays.[14]

In this article, we report the results of a comparative study on electrical and mechanical behaviour of composites prepared using a commercially available masterbatch from Hyperion, consisting of polypropylene loaded with 20 wt % of multi-walled CNT (MWNT), which was diluted with various types of polypropylene. The use of masterbatches for nanocomposites preparation is very convenient for many industrial applications; however, it is a bit problematic for fundamental research because of a lack of knowledge on nanotube and polymer properties and the protocol for masterbatch preparation. Even if some articles were published during the last years focussing on properties of nanocomposites prepared by masterbatch dilution,[15–21] no systematic study was done to investigate the use of different diluting polymers.[22]

Polypropylene is a nonpolar partial crystalline polymer and it is reported that it is more difficult to disperse nanotubes in this material as compared to amorphous polar polymers like polycarbonate. Due to only low interactions between polypropylene and nanotubes the primary nanotube agglomerates are difficult to disperse leading to higher percolation concentrations. Due to the partially crystalline structure a more gradual increase in conductivity is observed as compared to the sudden increase observed in amorphous materials[22,23]

In this study, the influence of the melt viscosity and of the modification of polypropylene with maleic anhydride on the dispersion and properties of CNT composites is investigated. For this, two sets of non-modified and maleic anhydride-grafted PP with different molecular weights, resulting in different melt viscosities, were selected. In addition, the polypropylene as applied in the masterbatch was also used for composite preparation. Modification with maleic anhydride is commonly used for polyolefins to introduce hydrophilic groups into the originally hydrophobic matrix with the aim to improve the compatibility with hydrophilic fillers.[24] Obviously, maleic anhydride does not react covalently with graphene sheets of CNT, however, maleated polyolefins have much higher adhesion to the polar substrates than unmodified ones.[25] Therefore, improvements in the nanotube dispersion and adhesion between PP and CNT can be expected.

This study also includes the comparative investigation on the crystallization kinetics and thermal, rheological, and mechanical properties of the composites based on the various grades of polypropylene mixed with the masterbatch. The phenomena of charge transport in composites below and above percolation threshold are also reported. The

TABLE I
Molecular Characteristics of Used PP Matrices and the Crystallinities of Prepared Composites

	PP_{12}	PP_8	PP_2	PP-MA_8	PP-MA_2
Young's modulus [MPa]	1070 ± 41	972 ± 1	939 ± 20	435 ± 18	450 ± 33
Stress at break [MPa]	33.8 ± 3.7	40.9 ± 3.3	42.7 ± 2.7	22.8 ± 4.7	27.1 ± 0.7
Strain at break [%]	737 ± 52	937 ± 78	996 ± 60	806 ± 111	984 ± 24
M_w [g/mol]	311,500	310,600	427,600	337,400	379,400
M_n [g/mol]	50,700	68,000	73,100	53,300	58,200
Dispersity index	6.14	4.57	5.85	6.33	6.52
MFI	11.8	8	2	8	2
CNT content [wt %]		X_c [%]			
0.0	37.9	33.4	30.3	23.4	31.1
0.8[a]/ 1.0			31.9	16.2[a]	31.3[a]
1.5	39.1	34.1			
2.0				16.5	28.3
2.5/ 2.7[a]			33.2	16.6[a]	29.5[a]
4.0	39.9	35.9	34.2	17.7	29.4
8.0	40.7	32.5	35.6	25.8	35.6

[a] The amount of CNT in the case of maleated PP's.

morphology of the composites was investigated using scanning electron microscopy (SEM), and transmission electron microscopy (TEM).

EXPERIMENTAL PROCEDURES

Materials

The masterbatch used for this study was supplied by Hyperion Catalysis International, (Cambridge). It has the designation MB3020-01 (labelled as *PP-MB*) and is based on a PP having a melt flow index MFI (2.16 kg at 230°C) = 11.8 g/10 min, labelled as PP_{12}. The masterbatch contains 20 wt % of multi-walled carbon nanotubes (diameter 10–15 nm, length up to 10 μm, 8–15 walls, see www.fibrils.com). This granular masterbatch material was diluted towards lower CNT contents through mixing with various PP matrices.

Two grades of a maleic anhydride (MA) modified polypropylene, OREVAC PPC, labelled as PP-MA_2 (MFI = 2 g/10 min, density = 0.89 g/cm^3, melting temperature T_m = 151°C) and OREVAC 18,732, labelled as PP-MA_8 (MFI = 8 g/10 min, density = 0.89 g/cm^3, T_m = 134°C) from Arkema, France, were used. The amount of maleic anhydride determined by titration method was 0.13 wt % for PP-MA_8 and 0.14 wt % for PP-MA_2. The two grades of unmodified polypropylene with similar viscosity behaviour as the MA-modified were NOVOLEN 1106H, labelled as PP_2 (MFI = 2 g/10 min, density = 0.9 g/cm^3, T_m = 154°C) from Basell, Germany, and HD214CF, labelled as PP_8 (MFI = 8 g/10 min, density = 0.9 g/cm^3, T_m = 162– 166°C) from Borealis A/S, Denmark. Some characteristics of the PP are summarized in Table I.

PP/CNT composites preparation

The composites were prepared by mixing of maleated PP (OREVAC PPC or OREVAC 18,732) with certain amounts of MB3020-01 in the 30 mL mixing chamber of a Plasti-corder kneading machine PLE 331 (Brabender, Germany) at 190°C for 10 min at a mixing speed of 35 rpm. One millimeter thick slabs were prepared by compression moulding of the mixed composites using a laboratory hydraulic press SRA 100 (Fontijne, Netherlands) at 2.4 MPa and 190°C for 2 min. Specimens with the desired dimension were cut from the slabs for mechanical, dynamic-mechanical, and rheological testing.

Characterization techniques

Rheological measurements

Melt rheological measurements were performed under nitrogen atmosphere on an ARES oscillation rheometer using plate/plate geometry (diameter 25 mm gap ca 1 mm) at 190°C on samples previously compression moulded into the disk shape. Frequency sweeps were done after approximately 5 min temperature equilibration with increasing frequency (0.1–100 rad/s) followed by a sweep with decreasing frequency (100–0.04 rad/s); the second sweep was used for interpretation. Both sweeps showed good agreement. The strain was set between 0.1% and 1% and checked to be within the linear-viscoelastic range using strain sweeps. The PP matrices were analysed using the same treatment as it was used for the composite preparation.

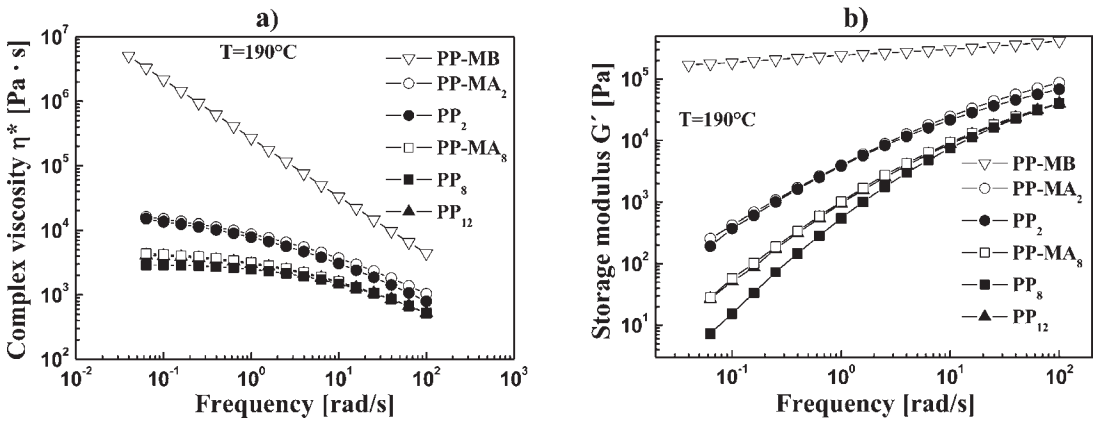

Figure 1 Complex melt viscosity (a), and storage modulus (b) at 190°C of the PP-MB and the polypropylene materials used for its dilution.

Morphological investigations

Scanning electron microscopy (SEM) and transmission electron microscopy (TEM) were used for direct observation of the CNT distribution in the PP matrices. For SEM, slabs were cryo-fractured after freezing in liquid nitrogen and the gold-sputtered fracture surface was analysed using an SEM LEO 435 VP (LEO Elektronenmikroskopie). The acceleration voltage was 10 or 15 keV.

TEM was performed on ca. 80 nm thin films that were obtained by ultra-microtomy at −120°C by means of an LEO 912 at 120 keV. The TEM analysis was done by the Polymer Service GmbH Merseburg, Martin-Luther-Universität Halle–Wittenberg.

Conductivity measurement

For Dielectric Relaxation Spectroscopy (DRS) measurements the complex dielectric permittivity $\varepsilon^* = \varepsilon' - i\varepsilon''$ was determined as a function of frequency (10^{-2}–10^6Hz) with an Alpha Analyzer (Novocontrol, Germany). The frequency-dependent ac conductivity σ_{ac} (actually real part of complex ac conductivity) was calculated from the measured dielectric loss ε''[26] by the following equation:

$$\sigma_{ac}(\omega) = \varepsilon_0 \cdot \omega \cdot \varepsilon''(\omega), \quad (1)$$

where $\varepsilon_0 = 8.85 \times 10^{-12}$ F·m^{-1} is the permittivity of the free space, and ω is the angular frequency. Golden circular electrodes were sputtered on both sides of the samples before measurement, to assure good electrical contact.

We used only dc conductivity σ_{dc}, what is the conductivity at zero frequency (at $\omega \rightarrow 0$).

Differential scanning calorimetry (DSC)

The thermograms of studied samples were obtained by a Pyris 6 calorimeter (Perkin Elmer) in the temperature range from −50°C to 180°C. Both heating and cooling were performed at a rate of 10 K/min and under nitrogen atmosphere. The mass of the samples varied from 4 to 10 mg. The crystallinity was calculated from curves obtaining during melting process except of PP-MA$_8$ series, where a crystallization peak was used. The crystallinities of the composites are normalized to the weight fraction of PP in the composites.

Mechanical properties

Mechanical properties were tested using universal tensile tester Instron 4301 (Instron) at a deformation rate 10 mm/min using dog-bone specimens 1 mm thick with a 35 × 3.6 mm^2 working area.

The thermal dependences of the storage modulus E' were determined by means of a DMTA instrument MKIII (Rheometric Scientific) in bending mode at a heating rate 2 K/min, frequency 10 Hz, in the temperature range from –50°C to 150°C using a 1 mm thick plate with a 9 × 8.5 mm^2 working area.

RESULTS AND DISCUSSION

Rheological properties of the different polypropylenes

It was the aim of the study to compare the effect of the maleic anhydride modification of PP on the dispersion and electrical percolation behaviour of the nanotubes. In order to see this effect, the PP materials with and without maleic anhydride should have a comparable melt viscosity which is reported to influence the dispersion behaviour of CNT in a polymer matrix.[22]

Even if the materials used for dilution were selected under the aspect to have similar melt flow index (MFI, measured at 230°C), melt rheological investigations over a frequency range should clarify the comparability of the materials used at the

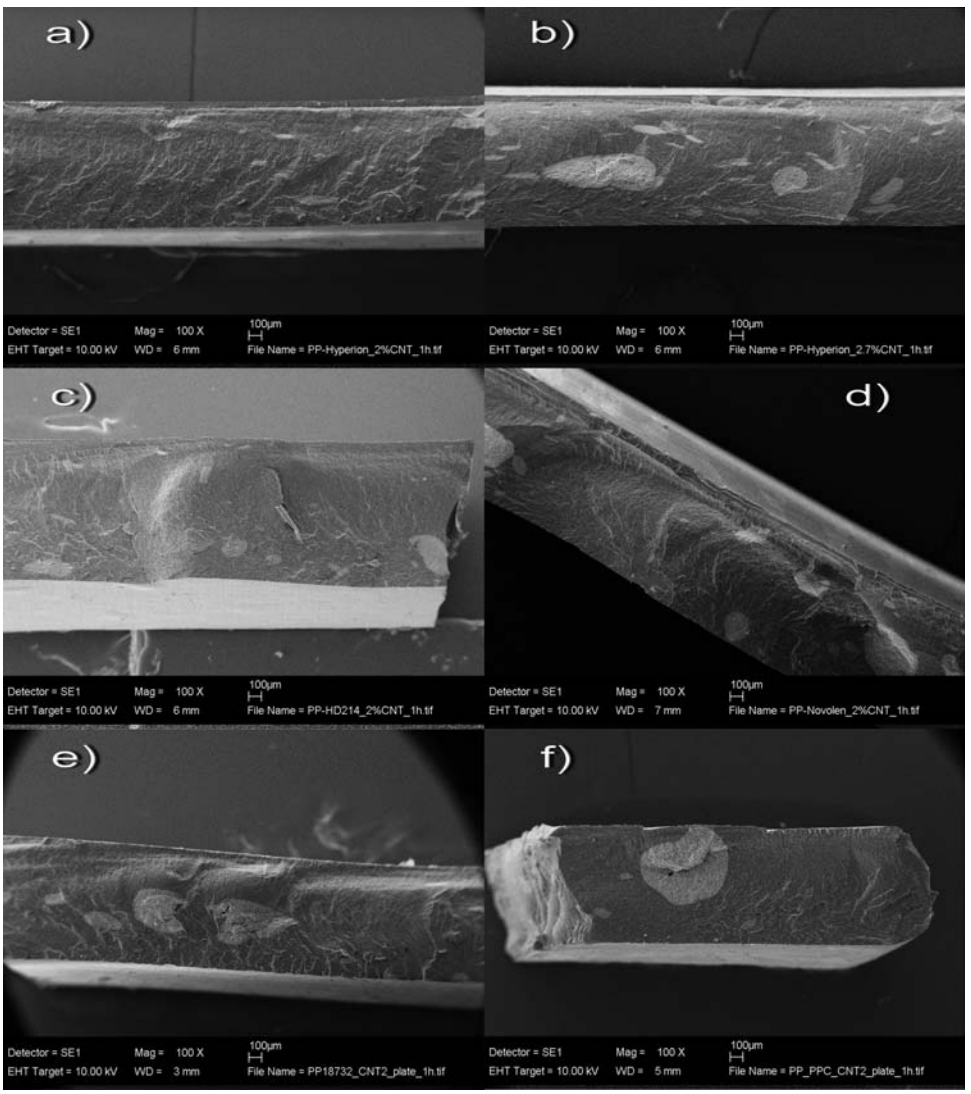

Figure 2 a) PP_{12} and CNT-agglomerates in different PP-CNT-composites containing 2.7 wt %, b) PP_{12} and 2 wt % CNT, c) PP_8, d) PP_2, e) PP-MA_8, and f) PP-MA_2 (SEM, cryo fractures, bar = 100 μm).

processing temperature of 190°C. Figure 1 presents the complex viscosities and storage moduli of the used PP matrices.

The figure illustrates that PP_2 and PP-MA_2 are comparable in both, viscosity and storage modulus as a measure for melt elasticity over the frequency range investigated. The maleated material has very slightly higher values. PP_8 and PP-MA_8 have significantly lower melt viscosities and storage moduli over the whole frequency range as compared to the PP_2 and PP-MA_2 as expected from the MFI values. The maleated material shows slightly higher values, especially at lower frequencies. Interestingly, PP_{12} has a higher viscosity at 230°C than PP_8 and it has the lowest values of storage modulus in this comparison. All PP materials show at low frequencies a Newtonian behaviour with nearly constant viscosities. The masterbatch material containing 20 wt % of MWNT (PP-MB) has very high viscosity values and a linear dependence of viscosity on frequency indicating the percolated state of the nanotubes. The viscosity differences to the diluting polypropylene materials are huge at all frequencies but increase with lower frequencies. The storage modulus of the same samples [Fig. 1(b)] shows only a slight decrease with decreasing frequency. This rheological study indicates that the two PP with MFI of 2 may be compared directly, and also both materials with MFI of 8 only show slight differences and may be compared. The PP with MFI 12 has viscosity and elasticity values similar to the maleated PP with MFI of 8. The materials with MFI of 2 are more similar to the masterbatch as compared to the materials with higher MFI.

Morphology of the composites

The masterbatch dilution technique is described in literature as a very convenient way to produce

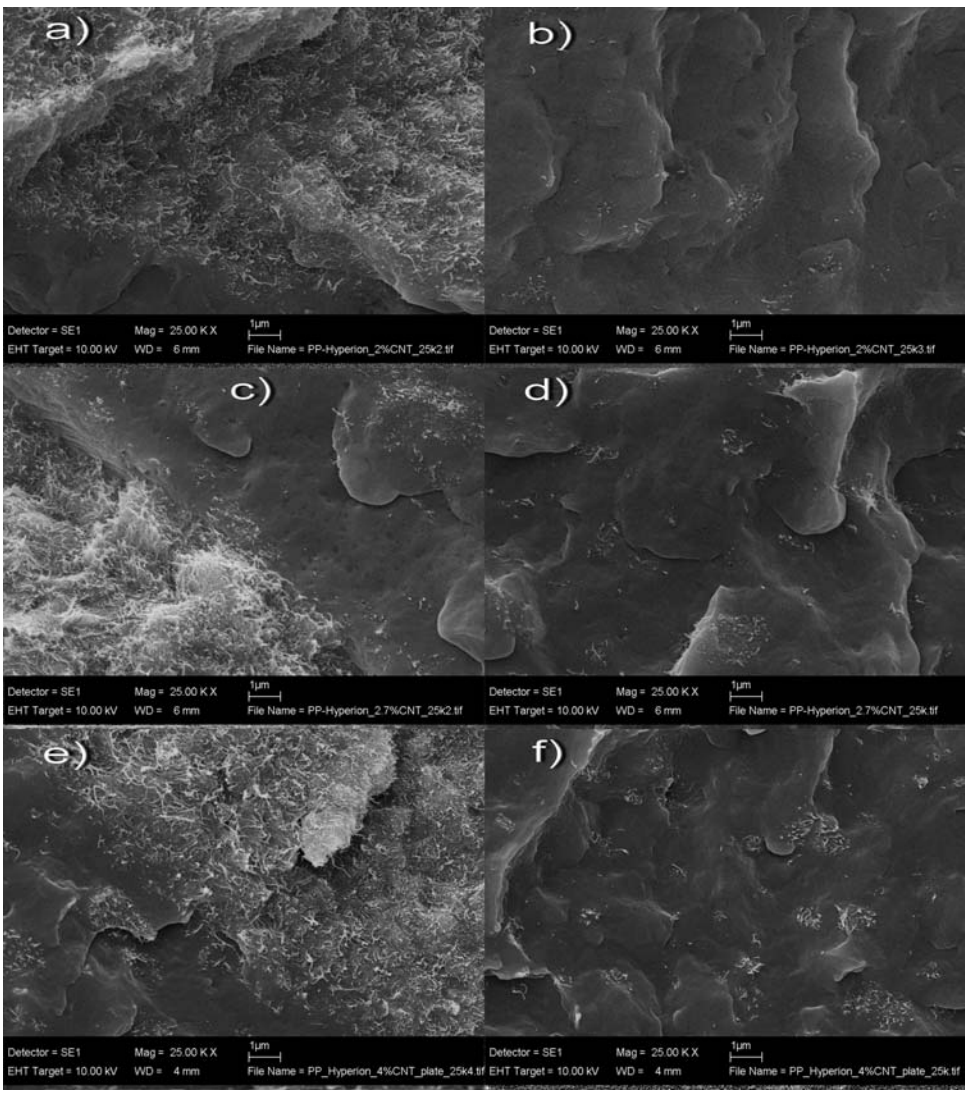

Figure 3 Interfaces between CNT-agglomerates and PP-matrix and distribution of small agglomerates and singularised CNT in PP_{12}-CNT-composites; a) and b) 2 wt % CNT, c) and d) 2.7 wt % CNT, e) and f) 4 wt % CNT (SEM, cryo fractures, bar = 1 µm).

nanocomposites. The nanotubes should be already wetted by the polymer matrix and the task is to gradually enhance the mesh size of the network by additional incorporation of matrix polymer and remaining the tube-tube contacts. For this, diffusion of diluting polymer chains inside the masterbatch network is needed which may be enhanced by low melt viscosity, high shear forces, and long mixing time. In addition, good interactions between the nanotubes and polymer chains may be favourable for homogeneous dispersion of the filler.

SEM images with low magnification (Fig. 2) show at the fractured surface in all composites, independent of the PP used for dilution, huge domains of agglomerated CNT in the dimension of some 100 µm as a result of inadequate dispersion, which are visible even with the naked eye. These agglomerates may be caused either by nanotube agglomerates already existing in the masterbatch which could be not dispersed anymore in the second mixing step or remaining masterbatch particles. Due to the broad size distribution of these domains no clear tendency in regard to the influence of the viscosity, MA-modification, or concentration on the domain size is visible, except the very big agglomerates in the case of PP-MA_2. However, quantification is impossible. The comparatively small domains in case of the sample PP_{12} with 2 wt % CNT (diluting with the same, low viscous PP as used in the masterbatch) seems to be an artefact caused by the statistic scatter since already the sample with 2.7 wt % CNT contains domains in the 500 µm range appear (Fig. 2b). Also light microscopy revealed bigger domains in the sample containing 2 wt % CNT.

With higher magnification, different areas can be recognized, which is exemplarily presented in Figure

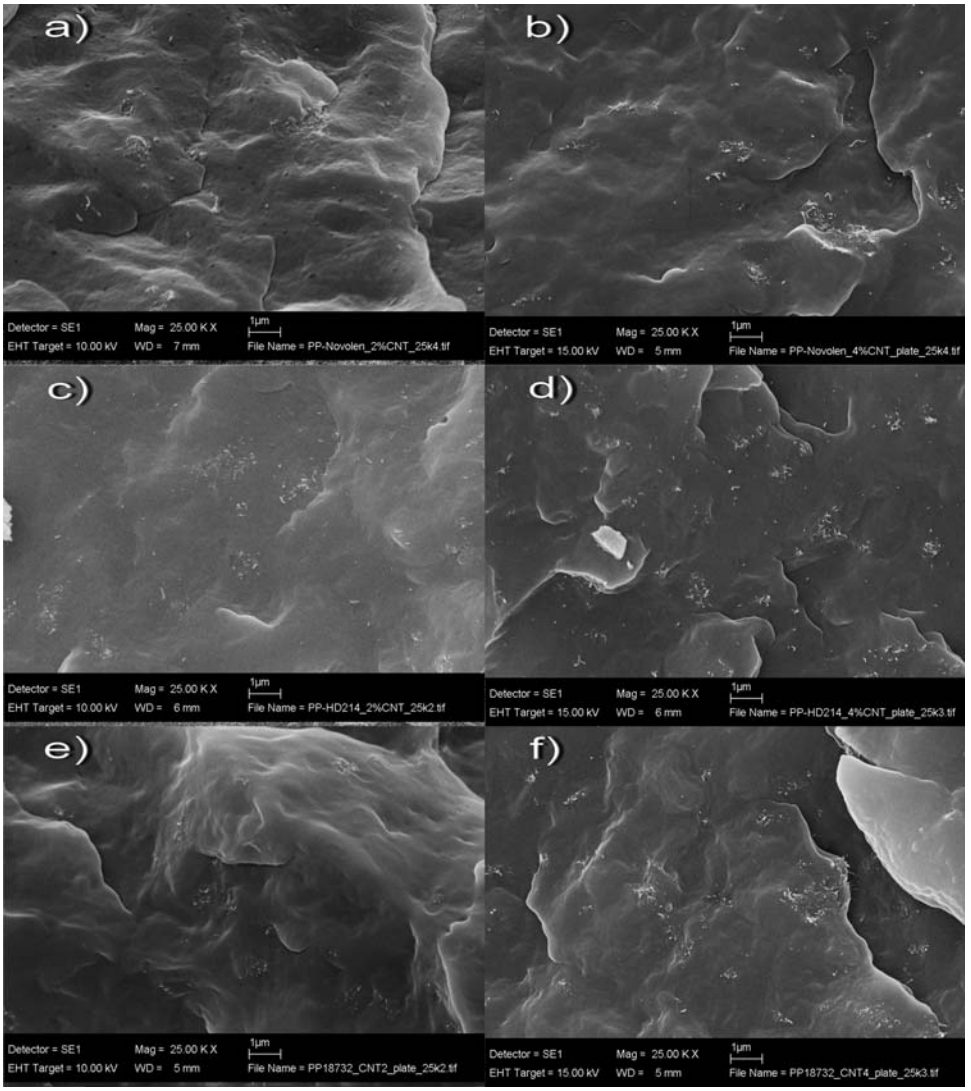

Figure 4 Dispersion of small aggregates and individualised CNT in different PP; a) PP_8-2% CNT, b) PP_8-4% CNT, c) PP_2-2% CNT, d) PP_2-4% CNT, e) PP-MA_8-2% CNT, f) PP-MA_8-4% CNT (SEM, cryo fracture, bar = 1 µm).

3 for the series prepared by dilution with PP_{12}. Beside the big domains smaller domains and more or less homogeneously dispersed single CNT are visible. The interface between the CNT-rich domains and the matrix is mainly diffused without a sharp gradient in composition. The increased concentration of small agglomerates next to the big agglomerates and the soft interfaces argue for an erosion mechanism, in which polymer penetrates from the surface into the big primary agglomerates. This results in increased mesh sizes, reduced CNT-CNT interactions, and a weakening of the surface layer of the agglomerates. Under shear stress this part can be removed from the agglomerate and dispersed in the polymer matrix. The sometimes observed sharp interface can be interpreted as area, where the softened part just has been removed. Although the erosion process of the big agglomerates starts again, the smaller and soft agglomerates can decompose further to smaller agglomerates or even individualized CNT.

Comparing the images with different CNT-content it becomes clear that the density of the small agglomerates increases with increased CNT-content. However, the influence of the PP-type on the agglomerate density hardly can be determined by SEM on cryofractures (Figs. 3, 4) since images with high magnification are presenting only very small sections of the whole volume. Furthermore, the fracture surface does not necessarily represent the mean characteristics of the morphology since the break will follow the weakest paths.

However, when PP-MA_2 is used for the composite preparation unambiguous differences in the morphology can be observed (Fig. 5). The PP-matrix appears as two phase system of two separated PP. Some PP of the masterbatch (which is not fixed in

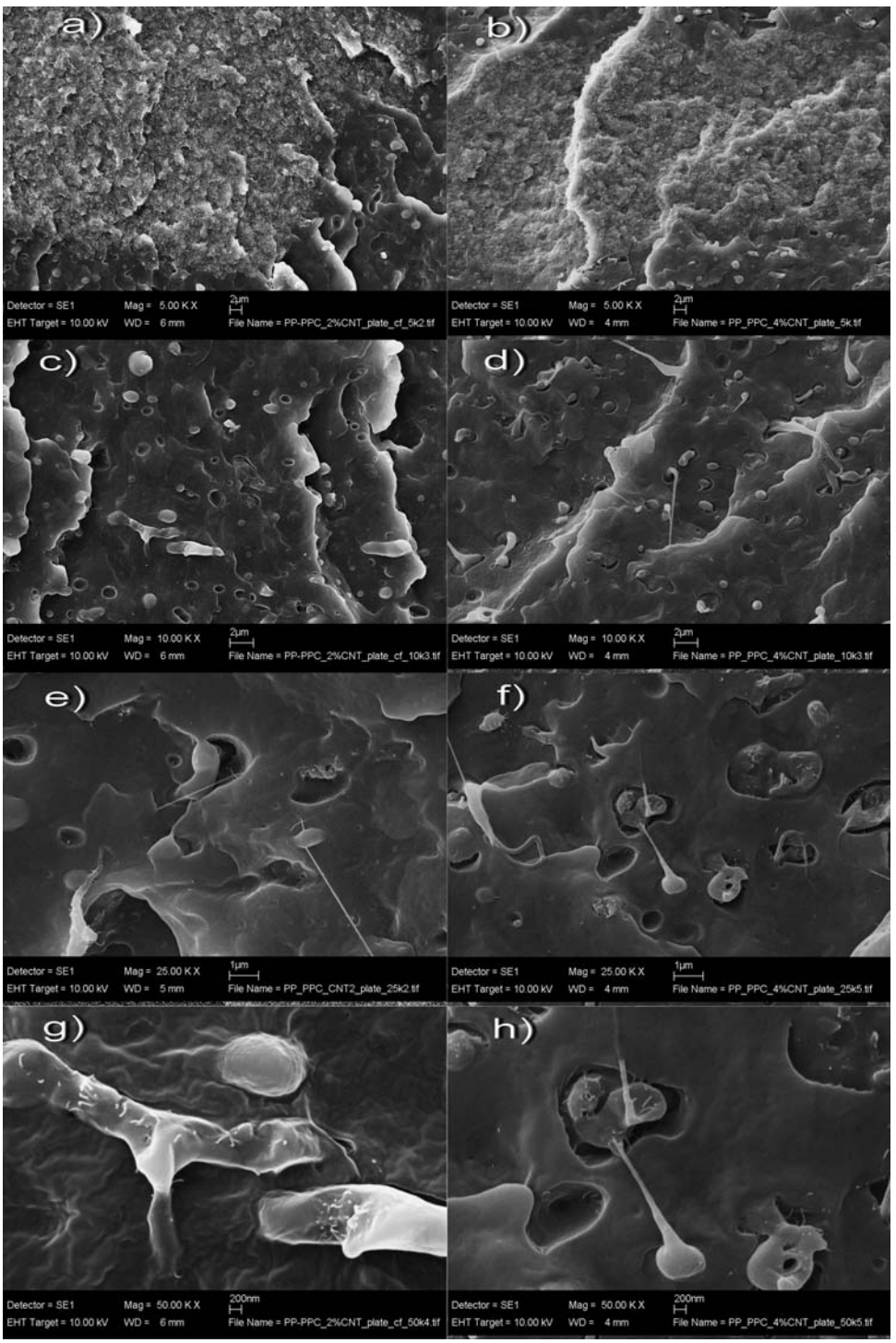

Figure 5 Three phase morphology of PP-MA_2-CNT composites containing a), c), e), g) 2 wt % CNT and b), d), f), h) 4 wt % CNT consisting of 100 µm-sized CNT agglomerates, dispersed masterbatch in µm-size, and PP-MA_2 matrix (SEM, cryo fracture).

the big primary agglomerate, Fig. 2) appears as small domains in roughly 1 µm dimension, homogeneously dispersed in the predominant PP-MA_2. The interfaces between the two PP-phases breaks partially during the cryofracture process resulting in good contrast in the SEM images. Even if most of the PP_{12} appears in circular shape the anisotropic shape of this phase is detectable. Furthermore it is evident that the dispersed PP_{12} phase contains almost all finely dispersed CNT, sometimes bridging the two PP phases. When not freezing the material completely, the low viscous PP_{12} containing most of the finely dispersed CNT deforms partially to long fibrils during the break, improving the contrast

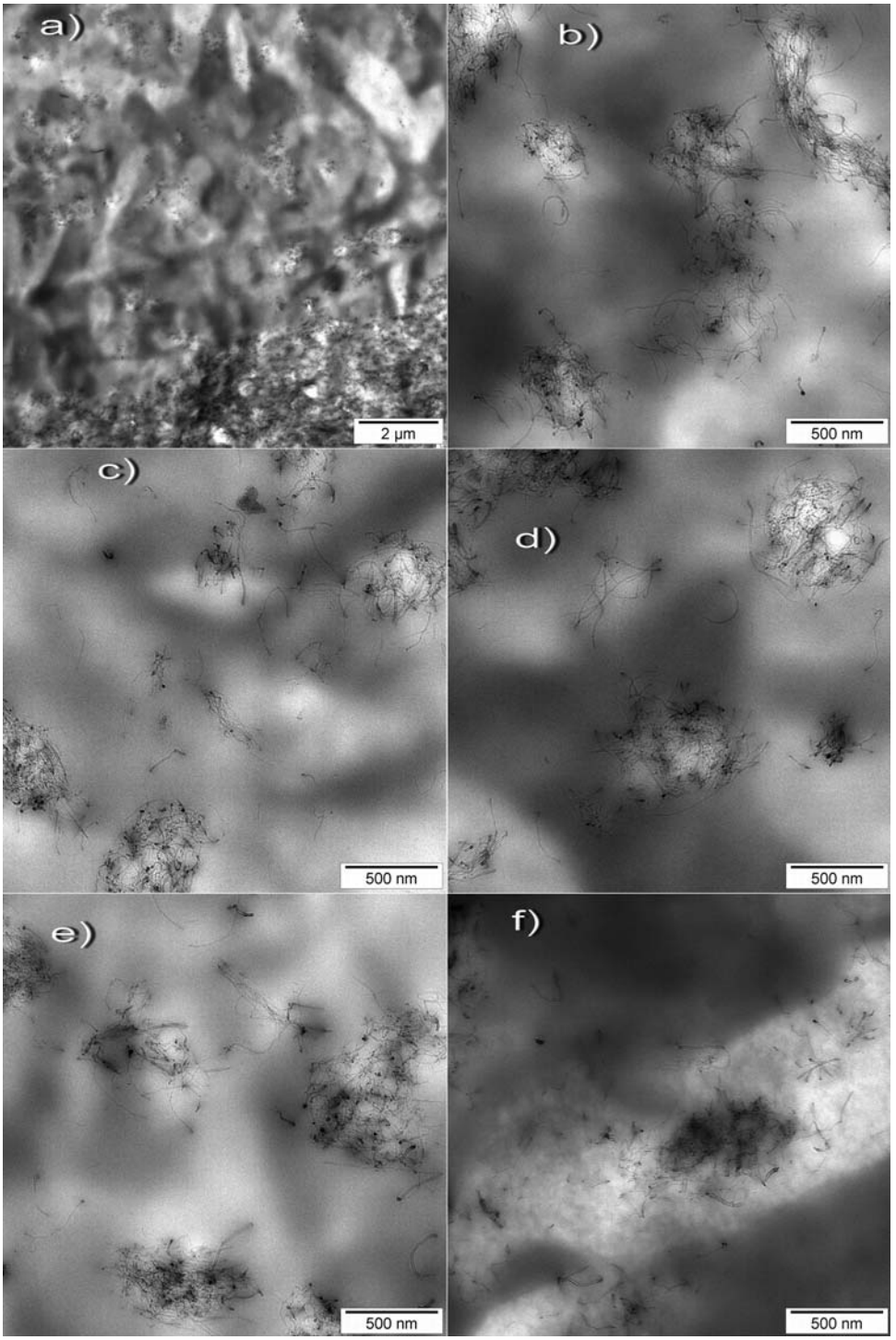

Figure 6 Distribution of the CNT in the PP-phase of different PP-CNT-composites (4 wt % CNT, TEM). a), b) PP_{12}; c) PP_8, d) PP_2, e) PP-MA_8, and f) PP-MA_2.

between the PP-MA_2 matrix and the dispersed masterbatch.

The appearance of two different PP-phases does not necessarily mean that both PP are thermodynamically immiscible. The process of homogenisation is just hampered due to differences in viscosity in combination with the presence of MA in the high viscous PP. In all other mixtures we did not find any signs for phase separation, except the presence of the big primary agglomerates.

TEM in low magnification also reveals the existence of bigger agglomerates (visible in the lower part of the first images in Fig. 6), but it is especially useful to analyse the dispersion and structure of small agglomerates and single CNT. In all samples agglomerates in the size of 500 nm to 2 µm are

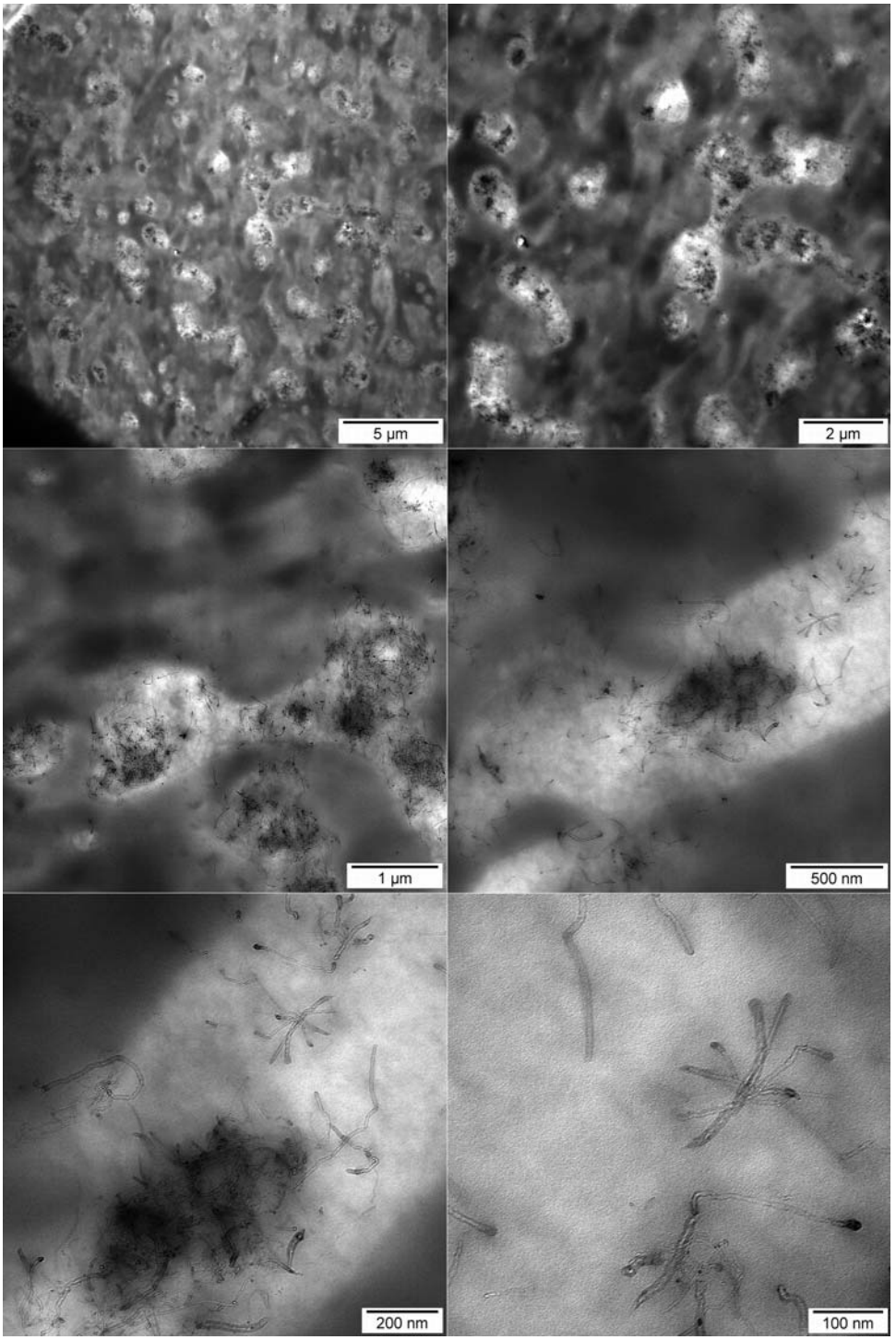

Figure 7 Morphology of PP-MA_2 (4 wt % CNT) separated into PP-MA_2 matrix poor on CNT and PP_{12}-CNT masterbatch containing CNT as agglomerates or individualized chains. Some CNT's are bridging between both phases (TEM).

detectable. Between these agglomerates smaller agglomerates and even single nanotubes exist (Fig. 6). In all samples agglomerates with different CNT densities (or CNT mesh sizes) can be found, representing different states of the dispersion process. Also inhomogeneities in the film thickness (the sample with PP-MA_2 was difficult to cut and is somehow thicker) may cause this effect. When comparing the samples containing 2 or 4 wt % CNT no significant differences in the size and density of the agglomerates are visible but the number of agglomerates increases with the CNT content. Therefore, we concentrate in this article on the samples with the higher CNT content. The main difference between

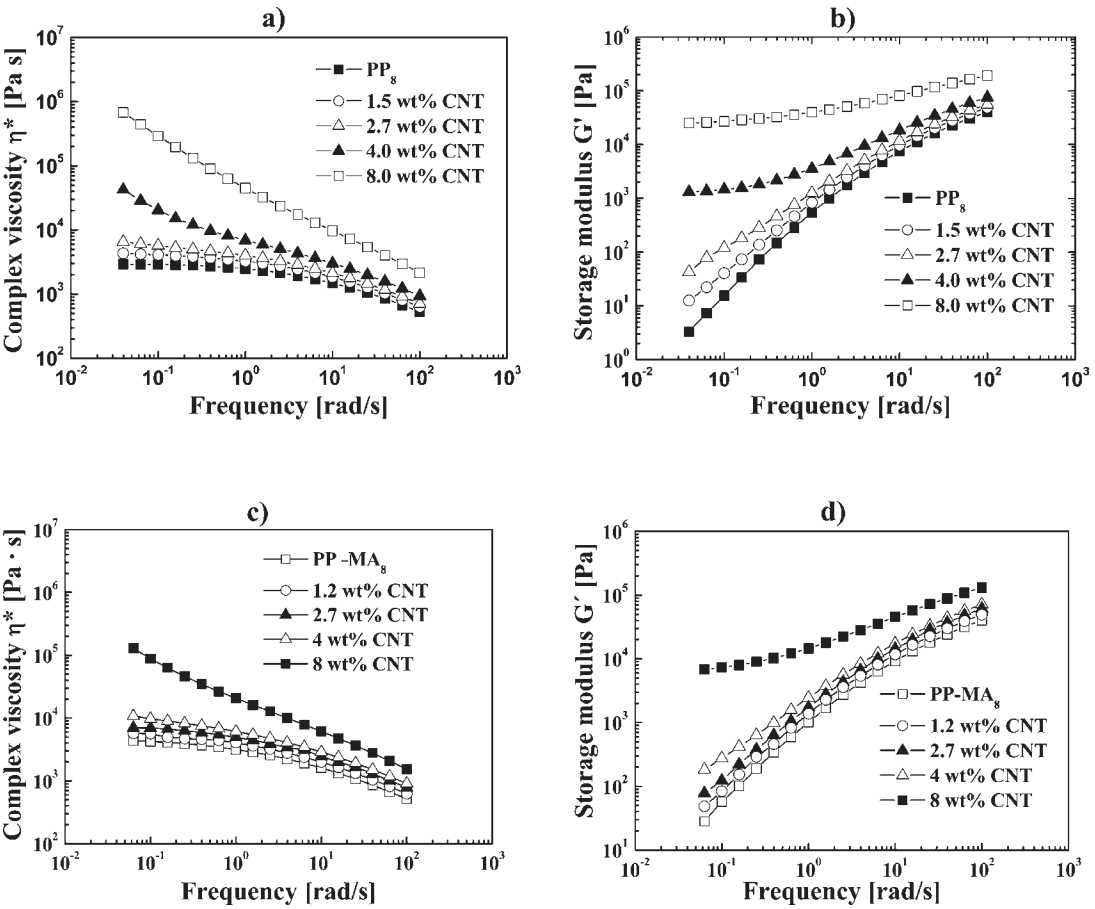

Figure 8 Complex melt viscosity (left) and storage modulus (right) vs. frequency at 190°C for composites based on PP_8 (a, b) and PP-MA_8 (c, d).

the samples is the bigger size of the observed agglomerates of up to 3 μm and the low content of individual CNT in case of the composites prepared with PP-MA_2.

A closer look to this sample reveals the coexistence of two different regions (beside the big primary agglomerates), one appearing more bright and containing almost all CNT in form of small aggregates and individual tubes, and one appearing more dark, in which only few nanotubes can be found (Fig. 7). This supports our SEM observations of a hindered miscibility between the masterbatch and the PP matrix. Some single nanotubes are crossing the interface indicating a diffusion from the masterbatch phase into the PP-MA_2 phase possibly driven by the better compatibility to the matrix with the higher polarity.

Although the length of the nanotubes can not be evaluated the observed, CNT-thickness of 7 to 16 nm correlates well with the literature data of 10 to 15 nm.

Rheological properties of the composites

The melt rheological properties of nanocomposites may serve as an indirect measure of the state of dispersion and network formation of nanotubes. It is generally accepted that interacting fillers in a polymer matrix lead to a Non-Newtonian behaviour at low measuring frequencies as indicated by a continuous increase in viscosity and the development of a plateau of the storage modulus by lowering the frequency. In composites based on layered silicates the determination of the slope of viscosity at low frequencies was proposed as a measure for the degree of exfoliation.[27]

The development of melt viscosity and storage moduli was studied for the different systems and is shown exemplarily for PP_8 and PP-MA_8 in Figure 8. The significant change in the rheological behaviour as described above, also named as "rheological percolation threshold," was observed at different nanotube contents for the different PP materials. For PP_2 and PP-MA_2 as well PP-MA_8 this was found between 4 and 8 wt % CNT, whereas for PP_8 and PP_{12} it occurred already between 2.7 and 4 wt % CNT content. In PP_8 exhibiting the lowest values in viscosity and storage modulus among the materials used the effect was most pronounced at this composition illustrating that dispersion may be best in this system. Up to the threshold values named here,

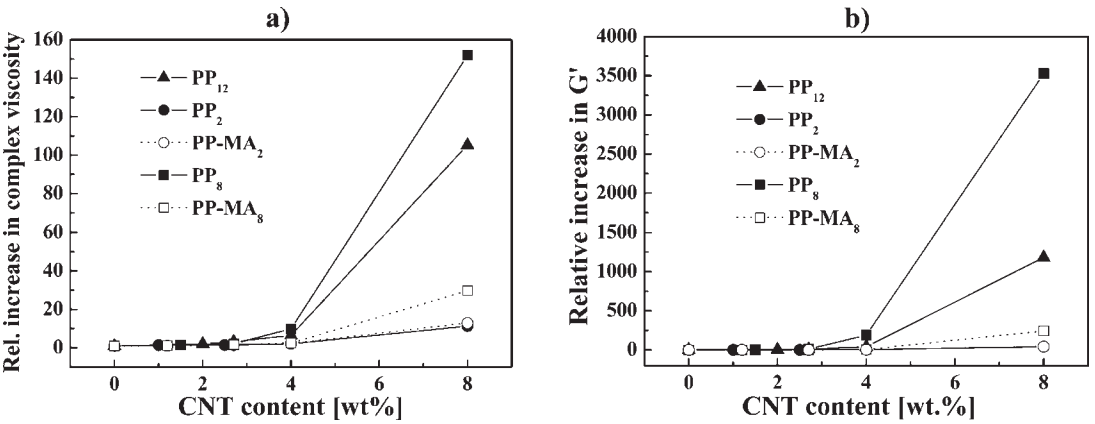

Figure 9 Relative changes (at a frequency of 0.063 rad/s) in complex melt viscosity (a) and storage modulus (b) vs. CNT content (values calculated by dividing nanocomposite values by the values of the matrix polymers).

only slight increases in viscosity and modulus occurred.

The relative increases in viscosity and storage modulus at a frequency of 0.063 rad/s (value of the composite divided by the value of the matrix) versus the CNT content are plotted in Figure 9. It indicates that the increase in storage modulus vs. CNT content is much higher than the increase in viscosity. For both types of PP having a MFI of 2 (maleated and nonmodified) the increases are similar and quite low, whereas the increases in composites based on PP_8 having MFI of 8 are much higher. Here, the maleated PP show much lower increases in viscosity and storage modulus as compared with the nonmodified one. The relative increases in viscosity and storage modulus of nanocomposites where with PP matrix used in the masterbatch (PP_{12}) are between those of PP_8 and PP-MA_8. Interestingly, this order follows exactly the order of melt viscosities of the pure PP materials, where PP_8 showed the lowest melt viscosity and storage modulus values in this comparison. This indicates that lower molecular chains can penetrate better inside the masterbatch and lead to better dispersion of the masterbatch particles as compared to longer chains as it is also illustrated by the occurrence of a rheological threshold at lower nanotube contents. However, it also illustrates that the relative stiffening effect is more pronounced if the polymer itself is less viscous (less stiff).

Mechanical properties

Since the degree of crystallinity has also the influence on the final mechanical properties of composites, we have confronted the crystallinity with mechanical properties. Table I summarizes the degree of crystallinity (X_c) of prepared composites obtained from DSC investigation of composites and PP matrices. As we can see the lower M_w (higher MFI) the higher the X_c, what is already observed phenomenon.[28] The X_c especially influenced the Young's modulus, since the crystallite region is stiffer than the amorphous phase. The highest absolute value of Young's modulus among the used matrices has PP_{12} (see Table I), since has the lowest molecular weight, what means the highest number of chain ends what consequently increase the nucleation density.[29] Maleinization generally decreased the X_c, since maleic groups hinders the stacking of PP chains.[30] This is obvious in the case of PP-MA_8, when is the lowest X_c as well as Young's modulus. Out of this considerations is the maleated matrix with MFI = 2, PP-MA_2. When compared with PP-MA_8 has higher M_w, but also higher X_c and when compared to MFI analogue PP_2 has higher X_c despite the presence of maleic group. It seems that in the case of PP-MA_2, the maleic group from some unknown reason is less active than in the case of PP-MA_8, since the extent of maleinization is in both cases the same, i.e., 0.14 and 0.13 wt % of maleic anhydride, respectively. Stress at the break of composites and its dependence on the filler fraction strongly depends on the type of PP as shown in Figure 10(a).

The stress at break of composites based on the PP_{12} matrix is not significantly influenced by the presence of the filler. It indicates that, in this case, the filler has no reinforcing effect on the matrix.[31] The other consequence is that, despite the fact that drawability of the composites drastically decreased even at the lowest filler content, it does not lead to the decrease of the strength; the feature that is commonly observed for polyolefin matrices.[32,33] The decrease of drawability of composites is shown in Figure 10(b). This figure displays the dependence of elongation at break on the filler content. It is seen that the drawability is drastically suppressed in the all investigated case even at the lowest filler content which lies in the interval from 0.4 to 1 wt %. There is only one exception observed, namely for composites based on the PP-MA_8 matrix. In this case,

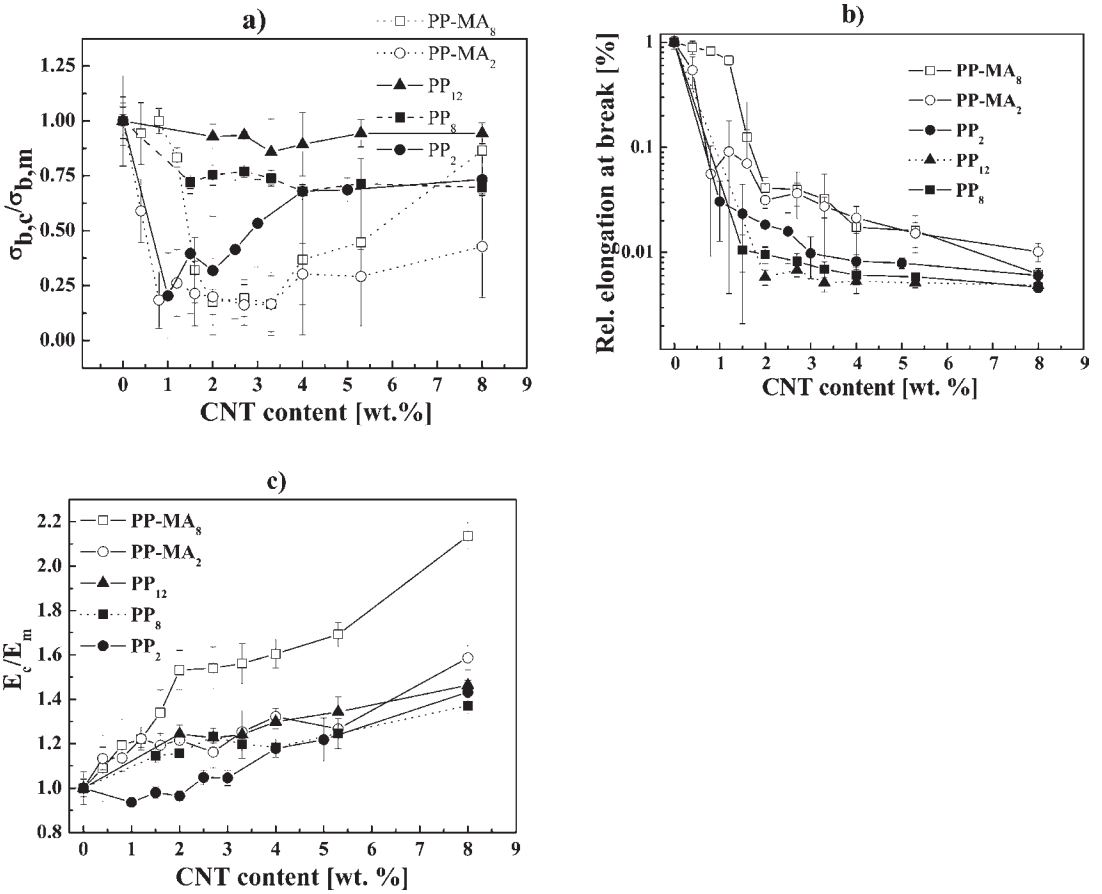

Figure 10 a) Dependences of relative stress at break ($\sigma_{b,c}$—stress at break of composite, $\sigma_{b,m}$—stress at break of PP matrix), b) dependences of relative elongation at break, and c) dependences of relative Young's modulus (E_c—Young's modulus of composite, E_m—Young's modulus of PP matrix) on the content of CNT of composites based on the PP_{12}, PP_8, PP_2, $PP\text{-}MA_8$, and $PP\text{-}MA_2$ matrices.

materials filled with 0.4, 0.8, and 1.2 wt % of CNT are very ductile, what is most probably caused by the increase of amorphous phase (decrease of X_c).

Different behaviour was observed for other matrices. The stress at break of composites based on the PP_8 matrix monotonously decreases with an increase in the filler content. It indicates insufficient interfacial interactions between the components.[31] Very unusual behavior was observed when PP_2 was used as the matrix. The initial decrease of stress at break is caused by suppression of both drawability and the orientation strengthening of the matrix.[32] However, a strong reinforcing effect of the filler was observed if the filler content was higher than 3 wt %. It was not expected effect since the PP_2 matrix is not chemically modified. In the case of $PP\text{-}MA_2$ and $PP\text{-}MA_8$ matrices the dependence of stress at break versus filler content varies nonlinearly. In this case, we have taken into account two influences of the filler on the stress at the break. On one hand, we have to consider the reinforcing effect of the filler leading to an increase in the tensile stress values with increasing of filler fraction because of improved interfacial interactions due to grafting by maleic groups, and, however, the orientation strengthening occurring for semi-crystalline polymers at high deformation.[31,32] The latter effect is indirectly negatively influenced by the filler presence and by a steep decrease of the deformation so that orientation of the matrix cannot occur. At low filler fractions, the deformation is low enough to prevent the orientation, but the reinforcing effect of the filler presence is marginal. The particles of the filler represent defects and stress concentrators.[33] The behavior of the stress-strain curve is changed; orientation hardening and cold flow is suppressed. The samples break close to the yield point. Therefore, an initial decrease of tensile strength has been observed. For instance, the initial stress at the break of $PP\text{-}MA_2$ (27.1 $\pm$ 0.8 MPa) decreased to the value of 16 $\pm$ 4 when it was filled with 0.4 wt % of the filler. The reinforcing effect is more pronounced with the increase in the filler fraction, while further decrease in deformation has no additional effect on orientation. The reinforcing effect becomes significant at the highest filler concentrations. This reinforcing effect is more pronounced in

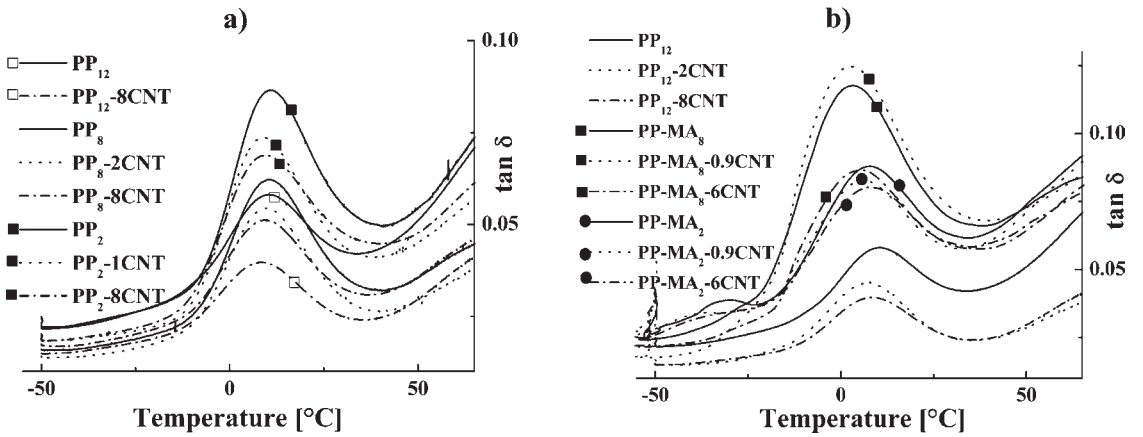

Figure 11 Temperature dependences of loss factor tan δ of composites prepared by using PP-MA_8, PP-MA_2, and PP_{12} matrices (a); and PP_8, PP_2, and PP_{12} matrices (b).

the case of PP-MA_2. This may be due to the different degree of crystallinity of these two matrices (31.1% for PP-MA_2 and 23.4% for PP-MA_8). In the case of PP-MA_8 matrix X_c even substantially decreased to 16.2% after adding a small amount of masterbatch. And since the filler is located only in the amorphous phase, the concentration of the filler relative to the amount of the amorphous phase is higher in PP-MA_2 than in PP-MA_8; consequently, the amorphous part of PP-MA_2 is more reinforced than PP-MA_8 due to a higher local concentration of the filler in this phase.[34]

The Young's modulus of composites monotonically increases with an increase in the filler fraction in the whole concentration region for the all used matrices. It is a common knowledge that the improvement in Young's modulus is an expected consequence of the reinforcing effect of the inorganic filler. It is known, that the improvement of tensile modulus depends not only on the Young's modulus of components but also is influenced by the good dispersion of particles and good interfacial adhesion between filler and the matrix.[35–37]

The dependencies of the relative Young's modulus on the CNT content are shown in Figure 10(c). It is seen that the maleinization improved the interfacial interactions between the components, especially in the case of PP-MA_8, what corresponds to the more active maleic anhydride group and thus better interaction on the boundary matrix-filler in this case.

The dependencies of loss factor (tan δ) on the temperature of the investigated composites are shown in Figure 11. The increase of loss factor in the case of PP-MA_8/0.9 CNT (Fig. 11a) could be ascribed to the decrease of X_c and thus to increase of amorphous phase contributing to segmental motions. In all other cases was observed the decrease of loss factor with the increase of carbon nanotubes, since the changes of the crystalline portion was not so pronounced and the presence of nanotubes constrain the amount of chain motions. A decrease of glass transition temperature (T_g) after adding small amount of CNT (0.9 wt %) in all cases was observed. The presence of nanotubes by obstructing the folding of polymeric chains induces an increase of free volume and consequently allows the cooperative motions of the polymer at lower temperatures.

In the case of maleated series it is worth to mention the peak around –30 °C (Fig. 11a). In the case of PP-MA_2 we can clearly see the release of side chains of maleic anhydride groups, but in the case of PP-MA_8 there is no peak at all. In the latter case is the maleic group probably in stronger interaction with the main chain. As a consequence are the properties of PP-MA_8 more influenced by the presence of maleic group than it is in the case of PP-MA_2.

TABLE II
Electrical Conductivities of PP/CNT Composites

Series	p_c [vol %]	CNT [wt %]	σ [S cm^{-1}]
PP-MA_2	1.26	2.7	4.20×10^{-13}
		3.3	1.40×10^{-4}
		8.0	3.20×10^{-3}
PP-MA_8	1.60	3.3	4.80×10^{-15}
		4.0	9.10×10^{-4}
		8.0	1.60×10^{-2}
PP_2	2.00	4.0	2.40×10^{-9}
		8.0	6.50×10^{-3}
PP_8	1.10	2.7	3.00×10^{-5}
		3.3	4.00×10^{-5}
		4.0	7.60×10^{-5}
		5.3	2.50×10^{-3}
		8.0	3.20×10^{-2}
PP_{12}	1.18	2.0	2.40×10^{-4}
		2.7	4.70×10^{-5}
		3.3	2.20×10^{-3}
		4.0	2.20×10^{-3}
		5.3	5.30×10^{-3}
		10.7	4.60×10^{-2}

Electrical percolation behaviour

Conductivity of the used masterbatch is 2.7 S cm^{-1}. Table II shows conductivity of all prepared nanocomposites and the calculated percolation thresholds. Percolation thresholds were calculated with following equation:

$$\sigma_c = \sigma_f(\Phi_f - \Phi_c)^t, \quad (2)$$

where σ_c, σ_f is conductivity of composite and the filler, respectively; Φ_f is volume ratio of filler and Φ_c is percolation concentration of the filler. The corresponding wt % concentrations can be then obtained using the density of carbon nanotubes $\rho = 1.8$ g/cm^3. In a simplified approximation wt % = 2 vol %. Electrical percolation confirmed the rheology results that best dispersion was achieved by PP_{12} and PP_8. From that it is clear that when using PP with lower viscosity for masterbatch dilution, better wetting and consequently a better CNT dispersibility were achieved. Also that higher shear forces during mixing applied when more viscous matrices were used is less significant. MA-modification was apparently not helpful for CNT dispersibility, since the improved interaction between matrix and nanotubes was overcoming by the incompatibility with the masterbatch PP. The highest value of percolation threshold 2.0 vol % of CNT, was achieved when PP_2 matrix was used for dilution the masterbatch. In this case is the largest difference in the M_w when compared with masterbatch PP_{12} matrix. This indicates that the larger polydispersity deteriorates the dispersion of the filler throughout the polymeric matrix. Work is in hand to examine electron transfer in studied composites and its relation to the nucleation ability of CNT in different PP matrices.

CONCLUSION

The results demonstrate that the masterbatch dilution technique is a suitable method to produce nanocomposites. The type and viscosity of the diluting polymer plays an important role on the dispersion of CNT in the matrix. With the maleinization we have achieved better interaction between polymer matrix and CNT, but the better dispersion was prevented by the incompatibility between polar groups of PP-MA and the nonpolar origin masterbatch PP_{12}. The best dispersion, as showed by percolations thresholds, rheology as well as from AC conductivity measurements, were achieved by PP_{12} and PP_8. This indicates that lower molecular chains can penetrate better inside the masterbatch and lead to better dispersion of the masterbatch particles as compared to longer chains. The matrix PP_8 has also similar M_w as the matrix of masterbatch PP_{12} (310,600 g/mol for PP_8 and 311,500 g/mol for PP_{12}) and the increase of polydispersity index in other cases could be the reason for inappropriate dispersion of CNT.

However, it has to be mentioned that remaining primary agglomerates in the masterbatch could not be dispersed effectively in the diluting step. The erosion mechanism works rather slow and the processing has to be modified to decompose the primary agglomerates completely. However, the shear forces, processing time, and temperature can not be increased too much due to matrix stability reason. Thus, high quality masterbatches with excellent nanotube dispersion are an essential requirement for high-quality diluted products.

References

1. Yu, F.; Files, B. S.; Arepalli, S.; Ruo, R. S. Phys Rev Lett 2000, 84, 5552.
2. Wagner, D.; Lourie, O.; Feldman, Y.; Tenne, R. Appl Phys Lett 1998, 72, 188.
3. Calvert, P. D. Nature 1999, 399, 210.
4. Carren, S. A.; Ajayan, P. M.; Blau, W. J.; Carroll, D. L.; Coleman, J. N.; Dalton, A. B.; Davey, A. P.; Drury, A.; Macarthy, B.; Maier, S.; Strevens, A. Adv Mater 1998, 10, 1091.
5. Chen, R. J.; Zhan, Y. G.; Wang, D. W.; Dai, H. J. J Am Chem Soc 2001, 123, 3838.
6. O'connell, M. J.; Boul, P.; Ericson, L. M.; Huffman, C.; Wang, Y. H.; Haroz, E.; Kuper, C.; Tour, J.; Ausman, K. D.; Smalley, R. E. Chem Phys Lett 2001, 342, 265.
7. Lin, Y.; Zhou, B.; Shiral, Fernando, K. A.; Liu, P.; Allard, L. F.; Ping Sun, Y. Macromolecules 2003, 36, 7199.
8. Funck, A.; Kaminsky, W. Comp Sci Tech 2007, 67, 906.
9. Xiao, K. Q.; Zhang, L. C.; Zarudi, I. Comp Sci Tech 2007, 67, 177.
10. Sandler, J. K. W.; Kirk, J. E.; Kinloch, I. A.; Shaffer, M. S. P.; Windle, A. H. Polymer 2003, 44, 5893.
11. Kovacs, J. Z.; Velagala, B. S.; Schulte, K.; Bauhofer, W. Comp Sci Tech 2007, 67, 922.
12. Schueler, R.; Peterman, J.; Schulte, K.; Wentzel, H. P. J Appl Polym Sci 1997, 63, 1741.
13. Schueler, R.; Peterman, J.; Schulte, K.; Wentzel, H. P. Macromol Symp 1996, 104, 261.
14. Le Baron, P. C.; Wang, Z.; Pinnavaia, T. I. Appl Clay Sci 1999, 15, 11.
15. Pötschke, P.; Bhattacharyya, A. R.; Janke, A.; Goering, H. Comp Interface 2003, 10, 389.
16. Pötschke, P.; Fornes, T. D.; Paul, D. R. Polymer 2002, 43, 3247.
17. Meincke, O.; Kaempfer, D.; Weickmann, H.; Friedrich, C.; Vathauer, M.; Warth, H. Polymer 2004, 45, 739.
18. Lin, B.; Sundararaj, U.; Pötschke, P. Macromol Mater Eng 2006, 291, 227.
19. Alig, I.; Lellinger, D.; Dudkin, S. M.; Pötschke, P. Polymer 2007, 48, 1020.
20. Peoglos, V.; Logakis, E.; Pandis, C.h; Pissis, P.; Pionteck, J.; Pötschke, P.; Mičušik, M.; Omastová, M. J Nanostruct Polym Nanocomp 2007, 3, 116.
21. Lee, S. H.; Kim, M. W.; Kim, S. H.; Youn, J. R. Eur Polym J 2008, 44, 1620.

22. Pötschke, P.; Pegel, S.; Janke, A.; Kretzschmar, B. Carbon Nanotube Filled Thermoplastic Polymers for Conductive and Antistatic Applications, VDI-Berichte Nr. 1920; Nanofair 2005, p 209, ISBN 3-18-091920-5
23. Pötschke, P.; Pegel, S.; Claes, M.; Bonduel, D. Macromol Rapid Comm 2007, 29, 244.
24. Page, D. J. Y. S.; Gopakumar, T. G. Polym J 2006, 38, 920.
25. Novák, I.; Krupa, I.; Janigová, I. Carbon 2005, 43, 841.
26. Kremer, F.; Schoenhals, A. Broadband Dielectric Spectroscopy; Springer: Germany, 2002, p 245.
27. Wagener, R.; Reisinger, T. J. G. Polymer 2003, 44, 7513.
28. Isayev, A. I.; Catignani, B. F. Polym Eng Sci 1997, 37, 1526.
29. Moon, C.-K. J Appl Polym Sci 1998, 67, 1191.
30. Henry, G. T. R. P.; Drooghaag, X.; Rousseaux, D. D. J.; Sclavons, M.; Devaux, J.; Marchand-Brynaert, J.; Carlier, V. J Polym Sci Pol Chem 2008, 46, 2936.
31. Manson, J. A.; Sperling, L. H. In: Polymer Blends and Composites, Plenum Press: New York, 1976
32. Krupa, I.; Chodák, I. Eur Polym J 2001, 37, 2159.
33. Krupa, I.; Miková, G.; Novák, I.; Janigová, I.; Nógellová, Z.; Lednický, F.; Prokeš, J. Eur Polym J 2007, 43, 2401.
34. Mičušík, M.; Omastová, M.; Prokeš, J.; Krupa, I. J Appl Polym Sci 2006, 101, 133.
35. Nielsen, L. E. In: Mechanical Properties of Polymers and Composites, Marcel Dekker: New York, 1974; p 2.
36. Nielsen, L. E. Trans Soc Rheol 1969, 13, 141.
37. Ferrigno, T. H. Polym Eng Sci 1978, 18, 33.